

Chapter 6

Challenges in Blending the Diesel–Ethanol Blends Using Butanol as Co-solvent Along with Diesel for Replacing the Neat Diesel to Fuel Compression Ignition Engines Suitable for Low-Temperature Application



B. Prabakaran

6.1 Introduction

Renewable energy resources are the major available resources to replace diesel fuel and reduce the dependency of diesel fuel to fuel compression ignition (CI) engines. This is the reason for the researchers to find out a renewable source such as alcohols or biodiesels from various edible or non-edible oils to reduce the consumption of diesel by blending to fuel CI engines. Alcohols are better than biodiesels in terms of combustion efficiency and emissions when fueled in compression ignition engines. Utilization of biodiesel from edible resources as fuel will lead to lack of resource for food. Ethanol (Han et al. 2020) can be blended into diesel for fueling in diesel engine which can be manufactured from biomass. The author utilized ethanol into diesel engine in a dual-fuel mode up to 80% and tested for performance. Author concluded that although 80% blending of ethanol is possible for blending, the increase in the ethanol content increased the ignition delay and decreased the thermal efficiency. It was also reported that misfire occurred by fueling blends containing higher volume of ethanol (higher than 30%) into diesel engine. The limitations in using biodiesel (Shamun et al. 2018; Belgiorno et al. 2018; Mamat et al. 2019) as fuel were stated by the author and recommended for low volume of biodiesel (up to 20%) along with diesel in diesel engine. The author also stated that there was a significant decrease in power by the utilization of biodiesel into CI engine. This motivated the researchers to increase the focus on fueling the CI engines with alcohol-blended diesel instead of

B. Prabakaran (✉)

Department of Automobile Engineering, Hindustan Institute of Technology and Science, Chennai, Tamil Nadu, India

e-mail: b7prabakaran@gmail.com

© The Author(s), under exclusive license to Springer Nature Singapore Pte Ltd. 2021

107

P. C. Shukla et al. (eds.), *Alcohol as an Alternative Fuel for Internal*

Combustion Engines, Energy, Environment, and Sustainability,

https://doi.org/10.1007/978-981-16-0931-2_7

Table 6.1 Properties of fuels standard

S. No.	Property	Diesel	Ethanol	Butanol
1	Density (kg/m ³)	829	785	809
2	Kinematic viscosity (mm ² /s)	4.04	1.07	2.6
3	Calorific value (MJ/kg)	42.8	26.9	33.1
4	Heat of vaporization (MJ/kg)	0.84	0.92	0.43
5	Flammability limits, volume (%)	0.6	19	11.2
6	Flashpoint (°C)	74	13	35
7	Cetane number	50	8	25
8	Research octane number	15–25	129	96
9	Energy density (MJ/L)	45.5	19.6	29

biodiesel-blended diesel. The utilization of methanol is not found attractive as this is meant as poisonous. This paved a way to progress to the next lower alcohol ethanol and its blend with diesel to fuel CI engine. Ethanol started its attempt as fuel for CI engines from 1980s onward. Compilation of previous researches for the utilization of diesel–methanol and diesel–ethanol blends (Kumar et al. 2013) into diesel engine was reported. The author conducted a study on the solubility, properties, and performance of these blends by fueling into CI engine. Table 6.1 shows the standard properties of diesel, ethanol, and butanol (Gao et al. 2019). From the table, the research octane number of ethanol is very much higher, this will lead to higher rate of combustion, and hence, ethanol has been chosen.

The author concluded that further research on the utilization of higher volume of ethanol in ethanol–diesel and higher volume of butanol in butanol–diesel blends can be further progressed in low-temperature analysis. Flame spread characteristics (Singh and Bharj 2019) of ethanol–diesel (containing 5% ethanol) in a CI engine have been compared with that of diesel. The author stated that the flame spread speed was found decreased at the initial phase and remains unchanged after certain height of ullage. This was due to the increase in the combustion efficiency and the rate of oxidation due to the higher oxygen content in the ethanol–diesel blends compared to that of diesel. A study was conducted by fueling 20% of ethanol along with *Jatropha* methyl ester and diesel blends on the evaporation characteristics in CI engine. It was reported that the liquid penetration and vapor penetration of the ethanol-blended biodiesel–diesel blends were found matching with that of diesel. The improvement in the evaporation rate of the fuel blend was due to the higher heat of vaporization of ethanol in the blend and the higher boiling point of the biodiesel in the blend. Ethanol was blended with diesel up to 19% and studied (Rakopoulos et al. 2019) for the essential properties such as cetane number, calorific value, sulfur content, and flashpoint. The author reported that the properties are found to be closer with respect to that of diesel fuel and suitable to fuel CI engine. The author also studied the performance and emissions characteristics of ethanol–diesel blends when fueled in CI engine. The report indicated that there was a significant increase in brake

thermal efficiency, decrease in the emissions and exhaust temperature by utilizing ethanol–diesel blend in CI engine. Cyclic irregularities of diesel–ethanol (Yu 2019) and diesel–butanol blends were compared when fueled in CI engine as fuel to replace diesel. The author stated that the cyclic variations produced by diesel–ethanol blends were found to be a bit stronger compared to those produced by diesel–butanol blends. The author stated that the reason for this activity was due to the fuel-bound oxygen possessed by ethanol in the blend. Most researchers attempted diesel–ethanol blends as fuel; however, attempts are limited for the fuel blend (Woo et al. 2016; Verma et al. 2018; Ribeiro et al. 2007; Hafid et al. 2017) possessing higher volume of ethanol and for low temperatures. Hence, this experimental study considers the objective as utilizing higher volume of ethanol under low temperature up to 5 °C with the assistance of n-butanol as co-solvent.

6.2 Materials and Methods

6.2.1 Fuels Used and Preparation of Blends

Diesel used in this study is Bharat Stage VI of low-sulfur diesel procured from market. Ethanol is procured from bioethanol producer who produces bioethanol (Stoeberl et al. 2011) from waste cut vegetables. These wastes are generally not utilized properly and thrown into garbage and causing land pollution to a greater extent. Biobutanol is procured from a bulk manufacturer who produces butanol from food (Hansen et al. 2005) wastages. **This is the novelty in this study.** To start with, biobutanol has been blended in proportions (Table 6.2) ranging from 0 to 10% in increments of 1% and kept separately. Table 6.2 lists the different proportions of diesel, ethanol, and butanol.

These biobutanol–diesel blends were taken in a beaker for blending of bioethanol. Bioethanol was filled in burette and slowly added into biobutanol–diesel blends in the proportions ranging from 0–50% in increments of 5% of bioethanol assisted with magnetic stirring. This was carefully handled such that bioethanol will not evaporate during the process of blending. The magnetic stirrer (Fig. 6.1) was operated at a speed of 1500 rpm and for a set cycle of 2 min.

Each blend has been stirred for three to five times, and the prepared blends were kept in a temperature-controlled box (Fig. 6.2) for five different temperatures 5, 10, 15, 20, and 25 °C. This temperature range has been chosen by considering the climatic conditions of India. In India, most part of the country (Prabakaran and Vijayabalan 2016) will attain 5 °C during the winter season. The fuel blend found by this study has to be suitable to fuel CI engine for most places in our country.

Fuel blends after the temperature stability tests are presented in Fig. 6.3. Figure 6.3 shows three representative samples kept at 5 (Fig. 6.5), 15 (Fig. 6.4), and 25 °C (Fig. 6.3) for a period of 20 days. Periodical monitoring has been performed, and the statuses of the blends were recorded. This is to find out the homogeneity of the fuel

Table 6.2 Various proportions of diesel–ethanol blends by varying butanol from 0–10%

Percentage of butanol	Fuels in percentage by volume										
1	D	94	89	84	79	74	69	64	59	54	49
	E	5	10	15	20	25	30	35	40	45	50
2	D	93	88	83	78	73	68	63	58	53	48
	E	5	10	15	20	25	30	35	40	45	50
3	D	92	87	82	77	72	67	62	57	52	47
	E	5	10	15	20	25	30	35	40	45	50
4	D	91	86	81	76	71	66	61	56	51	46
	E	5	10	15	20	25	30	35	40	45	50
5	D	90	85	80	75	70	65	60	55	50	45
	E	5	10	15	20	25	30	35	40	45	50
6	D	89	84	79	74	69	64	59	54	49	44
	E	5	10	15	20	25	30	35	40	45	50
7	D	88	83	78	73	68	63	58	53	48	43
	E	5	10	15	20	25	30	35	40	45	50
8	D	87	82	77	72	67	62	57	52	47	42
	E	5	10	15	20	25	30	35	40	45	50
9	D	86	81	76	71	66	61	56	51	46	41
	E	5	10	15	20	25	30	35	40	45	50
10	D	85	80	75	70	65	60	55	50	45	40
	E	5	10	15	20	25	30	35	40	45	50

D—Diesel, *E*—Bioethanol, *B*—Biobutanol

blend and to ensure that there is no phase separation between diesel and alcohols. The blends were also kept under 30 and 35 °C for 20 day. The blends are in the single liquid phase and no separation has been observe.

6.2.2 Testing the Properties of Fuel Blends

Prepared fuel blends (100 blends) were tested for the essential properties required as per the ASTM standards, and the properties were compared (Prabakaran et al. 2017) with respect to the diesel fuel as base. The instruments used for the properties along with the accuracy and ASTM standards are listed in Table 6.3. Table 6.4 lists the properties of five representative fuel blends (Prabakaran et al. 2019) containing 15, 25, 35, 45 and 50% of ethanol in comparison with that of diesel.

Fig. 6.1 Magnetic stirrer used for the blend preparation



Fig. 6.2 Temperature control box for storing the prepared blend in various temperatures





Fig. 6.3 Representative blends of diesel–ethanol with 10% *n*-butanol kept at 25 °C after 20 days

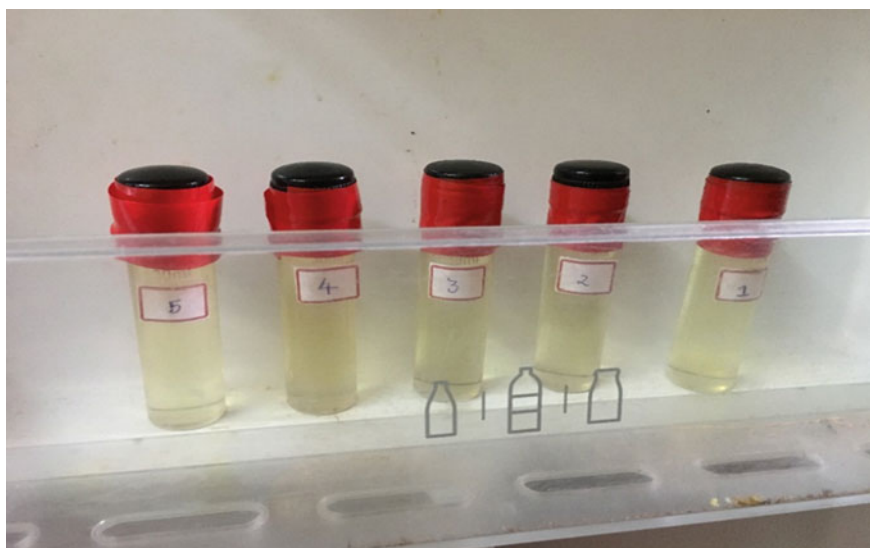


Fig. 6.4 Representative blends of diesel–ethanol with 10% *n*-butanol kept at 15 °C after 20 days



Fig. 6.5 Representative blends of diesel–ethanol with 10% *n*-butanol kept at 5 °C after 20 days

Table 6.3 List of instrument used for property testing

S. No.	Property	Unit	Instrument used	Accuracy	Percentage of uncertainty	ASTM standard
1	Flashpoint	°C	Pensky–Martens Closed cup	±0.1°C	±0.05%	ASTMD 93-16a
2	Kinematic viscosity	mm ² /s	Red wood viscometer	0.01 Centi Stokes	±0.02%	ASTMD445/446
3	Calorific value	kJ/kg	Bomb calorimeter	1 J/grams	±0.1%	ASTMD 4868
3	Cetane Number	No unit	Ignition delay	±0.1	±0.07%	ASTMD976/ASTMD4737

6.2.3 Experiment Setup

A single cylinder, four-stroke, water-cooled, direct injection, Kirloskar make diesel engine (Holman and Gajda 2001) of 4.4 kW capacity at the rated speed 1500 rpm was used for testing the fuel blends. The engine (Fig. 6.6) is coupled with eddy current dynamometer with electrical loading.

Fuel flow was measured with the help of burette and digital stop watch. Intake air flow was monitored by manometer and orifice plate. The displacement volume of the engine used was 661.5 cc, with a compression ratio of 17.5:1, and nozzle opening pressure was set at 200–205 bar. A provision was made for mounting the

Table 6.4 Properties of diesel–ethanol–butanol blends

Blend	Flashpoint	Energy content	Density	Kinematic viscosity	Oxygen content	Cetane number
Units	°C	MJ/kg	kg/m ³	mm ² /s	%	
Diesel	74	42.8	829	4.04	0	50
Ethanol	13	26.9	790	1.37	34.8	8
n-butanol	35	33.1	809	3.2	21.58	25
D75E15B10	64	40.24	823	3.7	5.64	43.3
D65E25B10	57.9	38.65	818	3.45	9.12	39.1
D55E35B10	51.8	37.06	813	3.19	12.59	34.9
D45E45B10	47.5	37.13	807	2.94	17.16	30.7
D40E50B10	39.6	33.88	805	2.62	19.6	26.5

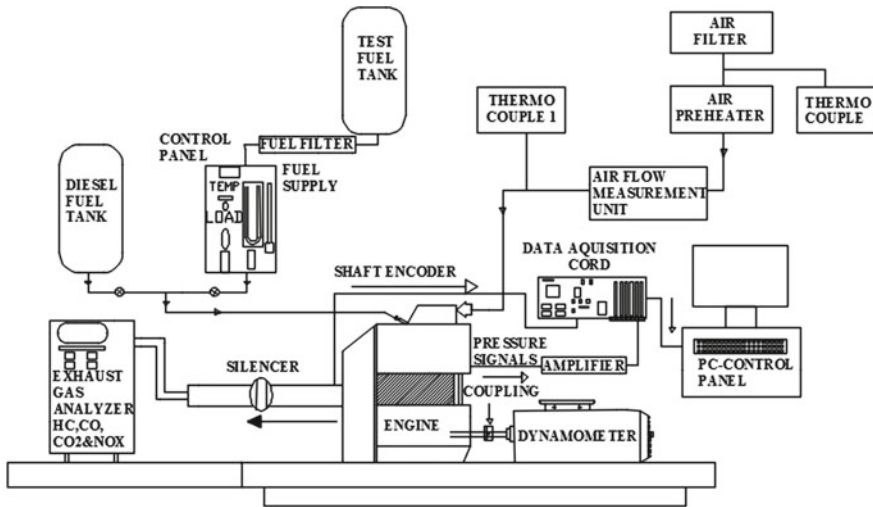


Fig. 6.6 Schematic layout of experimental setup

pressure transducer to capture the in-cylinder pressure signals during combustion and to feed the captured signals to the data acquisition device. The injection system of the experimental setup was mechanically controlled type, and this was periodically cleaned and calibrated as per the recommendations of the manufacturers. Air preheater is used to preheat the incoming air, and it is fixed in the suction side of the engine. In the present study, a heater of coil type of 1.0 kVA capacity is used for heating the incoming air. The temperature of the coil can be varied by varying the input electrical supply by a power regulator installed with the heater. The temperature of the incoming air to the air preheater and outgoing air from the air preheater has been measured by two separate thermocouple enabled with electronic readout. In the present study, a single, three-hole jet injector is deployed assisted by the mechanical

Fig. 6.7 Pressure calibration gage for fuel injector



centrifugal-type governor for injecting the fuel into the cylinder. The nozzle opening pressure is maintained at 200 bar. Variation of injection pressure was done by placing a washer of 0.20 mm for every 10 bar variation in between the nozzle and injector spring. The nozzle opening pressure was measured by calibrated gage with dial. The injector was clamped in the arms of the gage (Fig. 6.7), and the tripping fuel pressure was measured and indicated in the dial. This ensured the proper setting of the nozzle opening pressure. Normal injection timing is maintained at 23 °bTDC. Variation of injection timing was done by placing a shim of 0.25 mm (to attain 3° advance) between engine and fuel pump. The shim used has been calibrated and supplied by the manufacturer to attain the specified angle. Data acquisition system used for the present study consists of a computer, programmed with AVL 621 Indi-Modul system, which is receiving the signals amplified by a charge amplifier from a water-cooled pressure transducer of KISTLER piezoelectric transducer. This system was controlled by IndiCom software. Specifications of the pressure transducer are given in Appendix 4. This device was programmed for generating the combustion data according to the pressure input. Crank angle encoder captures the position of the crank angle of the respective pressure signal and was duly connected to the engine.

Hundred consecutive cycles of pressure data were captured and recorded for the analysis of combustion characteristics in the data acquisition system. This data acquisition system is programmed for combustion parameters calculation from the input received from the pressure transducer, crank angle encoder, and intake air measurement. This also receives the input from the thermocouples for the temperature of the intake air, exhaust gases, and in-cylinder. AVL-444 Di-Gas analyzer is used in this study for capturing the emissions from the test engine fuelled by the blends during the experiment. This measures CO, HC, NO_x, and CO₂ and oxygen concentration. It uses non-dispersive infrared (NDIR) sensor for measuring CO, CO₂, and HC.

Also, it measures NO_x and oxygen concentrations by electrochemical sensors. All the emissions are recorded and converted to g/kWh for further analysis. This device is auto-calibrated periodically as per the manufacturer advice. The measured values from the exhaust gas analyzer are in ppm (Gnanamoorthi and Devaradjane 2015), and the following conversion equations depict the conversion of ppm to g/kWhr which are standard equations (assuming 5% residual oxygen).

1000 ppm of NO_x corresponds to 6.60 g/kWh

100 ppm of HC corresponds to 0.20 g/kWh

100 ppm of CO corresponds to 0.36 g/kWh.

6.2.4 Experimental Uncertainty

Any experiment has its own uncertainty, and the overall uncertainty depends on the uncertainties of the various instruments used in the study and environment. In the present study, various instruments have been used, and each one has different level of uncertainty. This affects the final result. Hence, a detailed uncertainty analysis was carried out by the method of (Kuszewski 2018). The method implemented is recording five consecutive readings for each setting, and the average of these five readings was considered. The error included in these readings was found by using root mean square method. The maximum uncertainty of the experiment was arrived as $\pm 1.3\%$. The uncertainty in any measured parameter was estimated based on Gaussian distribution method with confidence limits of $\pm 2\sigma$ (95% of measured data lie within the limits of 2σ of mean). Thus, the uncertainty (Eq. (6.1)) was estimated using the following equation:

$$\text{Uncertainty of any measured parameter } (\Delta x_i) = (2\sigma_i / \bar{X}_i) * 100 \quad (6.1)$$

Experiments were conducted to obtain the mean (\bar{X}_i) and standard deviation (σ_i) of any measured parameter (X_i) for a number of readings. Engine was allowed to operate at a typical operating condition. The number of readings (minimum five readings) was taken for speed, load, temperature, pressure, exhaust gas emissions, and time taken for a specified volume of diesel consumption. Some of the measuring instruments and its ranges, accuracy, and the percentage of uncertainties are given at the end of this explanation. From the uncertainties of the measured parameters, the uncertainties in computed parameters are evaluated by using an expression, which is derived as follows. If an estimated quantity R depends on independent variable like ($x_1, x_2, x_3, \dots, x_n$), then the error in the value of “ R ” is given by equation

$$R = f(x_1, x_2, \dots, x_n) \quad (6.2)$$

with “ R ” as the computed result function of the independent measured variables $x_1, x_2, x_3, \dots, x_n$, as per the relation equation $x_1 \pm \Delta x_1, x_2 \pm \Delta x_2, \dots, x_n \pm \Delta x_n$ as

the uncertainty limits for the measured variables or parameters and the error limits for the computed result as $R \pm \Delta R$. To get the realistic uncertainty limits for the computed result, the principle of root mean square method (Eq. (6.3)) was used to get the magnitude of error given by Holman et al.

$$\Delta R = \left[\left(\frac{\partial R}{\partial x_1} \Delta x_1 \right)^2 + \left(\frac{\partial R}{\partial x_2} \Delta x_2 \right)^2 + \dots + \left(\frac{\partial R}{\partial x_n} \Delta x_n \right)^2 \right]^{1/2} \quad (6.3)$$

Using equation, the uncertainties in the computed values such as brake power, brake thermal efficiency, and fuel flow measurements were estimated. The measured values such as speed, load, fuel time, voltage, and current were estimated from their respective uncertainties based on the Gaussian distribution.

The estimated uncertainty values at a typical operating condition are given below:

Speed: $\pm 0.12\%$	Load: $\pm 0.49\%$
Mass flow rate of air: $\pm 0.62\%$	Mass flow rate of diesel: $\pm 0.87\%$
Brake power: $\pm 0.25\%$	Brake thermal efficiency: $\pm 0.27\%$
NO_x : $\pm 1.1\%$	Hydrocarbon: $\pm 0.01\%$
CO $\pm 0.8\%$	Smoke: $\pm 1.3\%$

There are various methods available to reduce the errors observed in the instruments such as selecting the instruments according to the measurement level required (range of measurement), accuracy of the instrument used, and sensitivity, and this experiment was conducted by deploying the appropriate instruments within the range of measurement, accuracy, and sensitivity requirement.

6.3 Results and Discussion

Cylinder pressure diagram with respect to crank angle is the indication of effect of in-cylinder combustion in an engine. Generally, cylinder pressure of any engine depends on the volatility of the fuel used, time duration of combustion, rate of heat release, and energy content of the fuel. It is seen from Fig. 6.8 that higher in-cylinder pressure is produced by blends D75E15B10 and D65E25B10 compared to diesel.

This is due to the improved complete combustion of the blends by the addition of ethanol to a certain extent. However, fuel blends D55E35B10 and D45E45B10 produce lesser in-cylinder pressure compared to diesel (Pinzi et al. 2018). This is due to the suppression of combustion by the higher volume of ethanol in the blends, which is due to higher heat of vaporization. It can also be observed from figure that the peak pressure from D75E15B10 and D65E25B10 is found to be higher by 6.4% and 15.2% compared to diesel. Figure 6.9 shows the variation of in-cylinder peak pressure versus brake power for the blends. It is seen that the addition of ethanol (up

Fig. 6.8 Variation of in-cylinder pressure versus crank angle

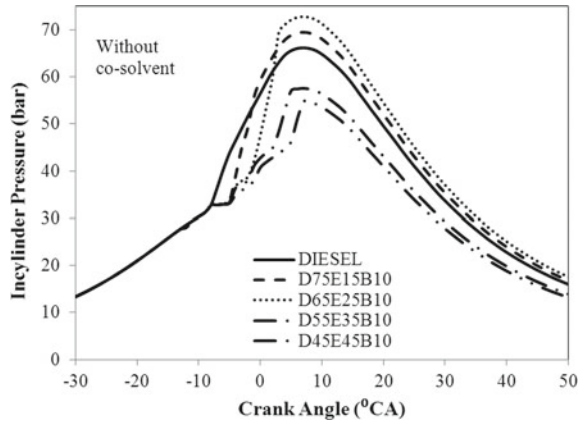
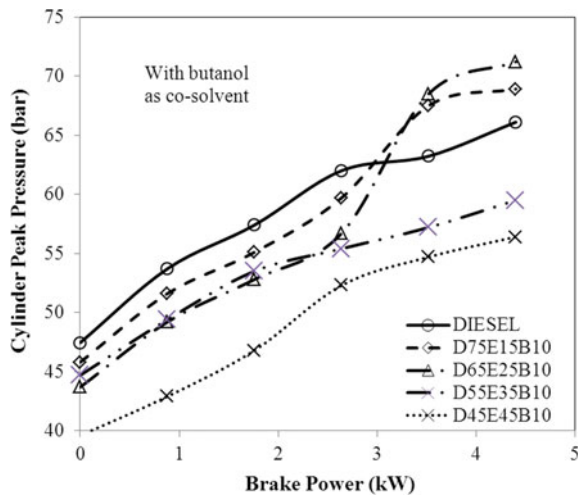


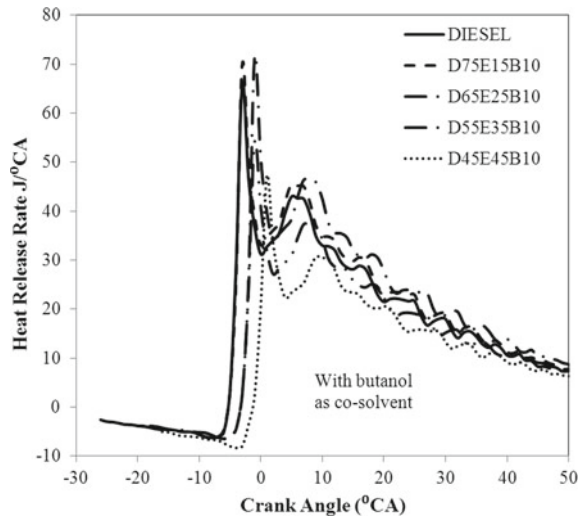
Fig. 6.9 Variation of in-cylinder peak pressures of diesel-ethanol-butanol blends



to a volume of 25%) into diesel increases the in-cylinder peak pressure significantly. Also, the increase in the in-cylinder peak pressure is found proportional to the increase in brake power. This is due to the improvement in the physico-chemical properties of the blends by the addition of ethanol. The improvement in kinematic viscosity (Yilmaz 2012) and density results in better atomization which leads to the more complete combustion.

It is also seen that the addition of ethanol into diesel (higher than 25% by vol.) reduces the in-cylinder peak pressure significantly. This is due to the dominance of heat of vaporization of the blends with the increase in the volume of ethanol (higher than 25% by vol.) in the blend. This produces a cooling effect which results in poor atomization and low rate of oxidation which results in lower in-cylinder peak pressure. The increases in in-cylinder peak pressure of D75E15B10 and D65E25B10

Fig. 6.10 Variation of HRR of fuel blends with crank angle at rated power

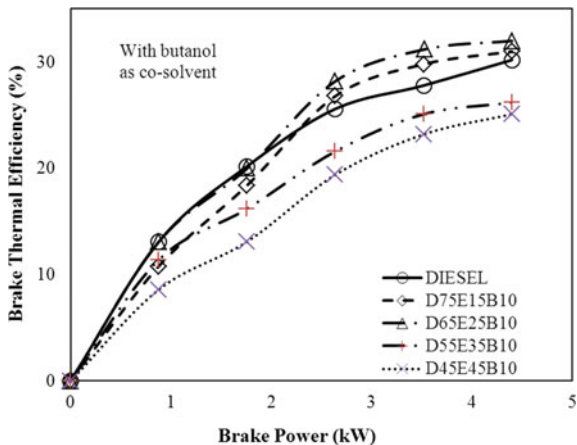


significantly. Also, the increase in the in-cylinder peak pressure is found proportional to the increase in brake power. This is due to the improvement in the physico-chemical properties of the blends by the addition of ethanol. Heat release rate is an indicator of combustion efficiency, and these parameters is helping for explaining the brake thermal efficiency (BTE), exhaust gas temperature, rate of pressure rise, emission parameters, and cylinder pressure.

Figure 6.10 shows the variation of HRR of fuel blends with 10% butanol as co-solvent without any modification under full load condition. HRR graphs are generated at all loads, and for representation HRR at full load condition is presented. It can be seen from figure that ethanol addition up to 25% increases the HRR to a greater extent due to the enhanced combustion behavior resulted from better atomization. However, the increase in ethanol content beyond 25% decreases HRR of the blends due to poor atomization which result in lower heat release rate. From figure, it is also seen that the blends containing lower ethanol offer higher HRR and blends containing higher ethanol offer lower HRR. The peak HRR of the blends occurs an angle away from that of diesel with respect to top dead center. The combustion duration of the blends containing lower ethanol is shorter than that of blends containing higher ethanol content.

The increases of HRR of D65E15B10 and D55E25B10 are found to be 8.8 and 12.9% higher compared to diesel (Verma et al. 2018). It can be observed from Fig. 6.11 that two (Ghadikolaei et al. 2018) blends D75E15B10 and D65E25B10 offered higher BTE compared to diesel at all load conditions. This is due to an increase in volatility and an improvement in spray characteristics of the fuel blends till the addition of 25% of ethanol into diesel. This results in higher BTE. However, for the two blends D55E35B10 and D45E45B10 produced lower BTE compared to diesel. This is mainly due to the decrease in self-ignition property of the final blend by the presence of higher volume of ethanol due to this increase in the heat

Fig. 6.11 Variation of brake thermal efficiency versus brake power



of vaporization. This increase in heat of vaporization produces cooling effect in the in-cylinder thereby reducing the temperature which in turn reduces the reactivity of oxygen with the fuel. The increases of BTE for D75E15B10 and D65E25B10 are found to be 4.1 and 9.2% higher compared to diesel at full load condition (Kuszewski 2018).

Also, the decreases of BTE for the blends D55E25B10 and D45E45B10 are found to be 1.9 and 2.6% lower than diesel. Variations of EGT versus brake power for the blends are presented in Fig. 6.12. It is seen that the EGT of the blends containing higher volume of ethanol produced a cooling effect by the dominance of heat of vaporization of the final blends. This produces a cooling effect in the in-cylinder

Fig. 6.12 Variations of exhaust gas temperature versus brake power

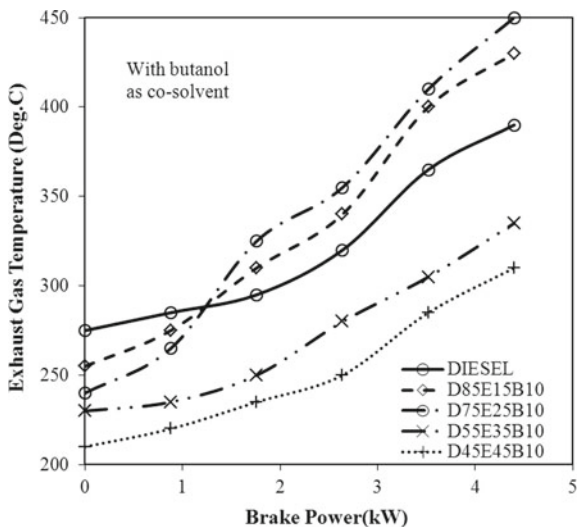
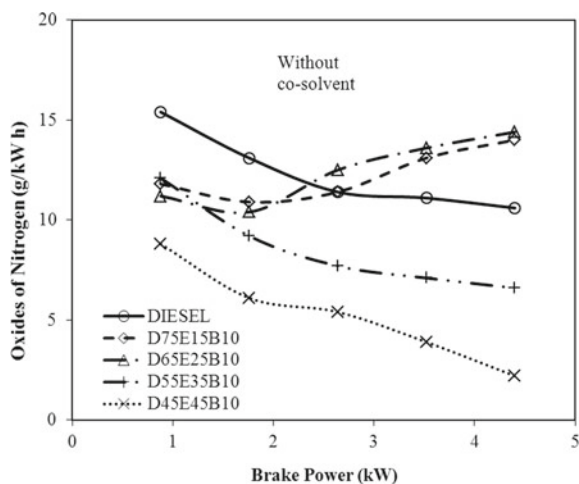
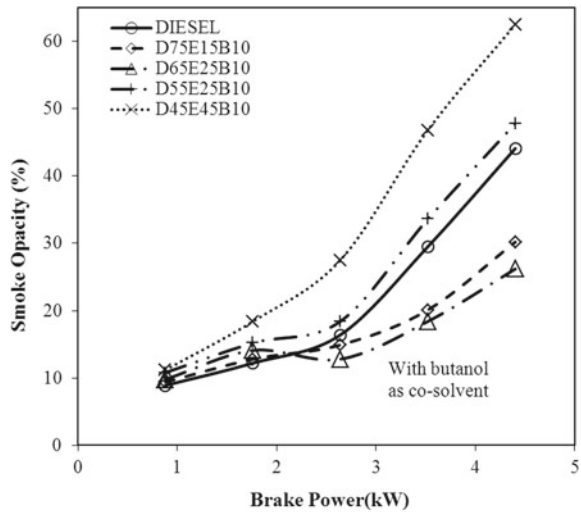


Fig. 6.13 Variation of NO_x emissions of fuel blends versus brake power



which reduces the rate of reaction of fuel particles with oxygen available in the in-cylinder and results in lower BTE and lower EGT. This is the main reason for the decrease in EGT of D55E35B10 and D45E45B10 (Rakopoulos et al. 2014). The increases of EGT for the blends D75E15B10 and D65E25B10 are found to be higher by 16.9% and 22.6%, respectively, compared to diesel at rated power. The decreases of EGT for the blends D55E35B10 and D45E45B10 are found to be 13.6% and 20.4%, respectively, compared to diesel at rated power. This emission from a CI engine is an indication of degree of complete combustion and higher temperature of the in-cylinder (as the formation of oxides of nitrogen is a higher-temperature reaction). From Fig. 6.13, it can be seen that the blends containing lower volume of ethanol (less than 25%) produce higher NO_x emissions and the blends containing higher volume of ethanol (more than 25%) produce lower NO_x emissions compared to diesel. This is mainly due to the higher temperature has been offered by the blends of lower ethanol content and lower temperature offered by the blends containing higher ethanol content. Also, the addition of ethanol up to 25% by volume improves the volatility, atomization of the fuel blends in the in-cylinder, and self-ignition property of the final blend. This is due the higher heat of vaporization of ethanol which suppresses the combustion temperature to a greater extent. D75E15B10 and D65E15B10 offer higher NO_x emissions and are found to be 2.6% and 7.6% higher compared to diesel. However, D55E35B10 and D45E45B10 offer significantly lower NO_x emissions compared to diesel (Rakopoulos et al. 2008). Smoke emissions from a CI engine are also an indication of low temperature of in-cylinder during combustion and the availability of oxygen for combustion of fuel. Figure 6.14 indicates the smoke emissions of blends containing 15, 25, 35, and 45% of ethanol with 10% butanol as co-solvent. From the figure, it is observed that D65E25B10 offers the lowest smoke emissions compared to those produced by other blends. This is due to the improved combustion characteristics of the final blend containing ethanol up to 25% by volume. More specifically, the addition of ethanol up to 25% by volume

Fig. 6.14 Variation of smoke emissions versus brake power

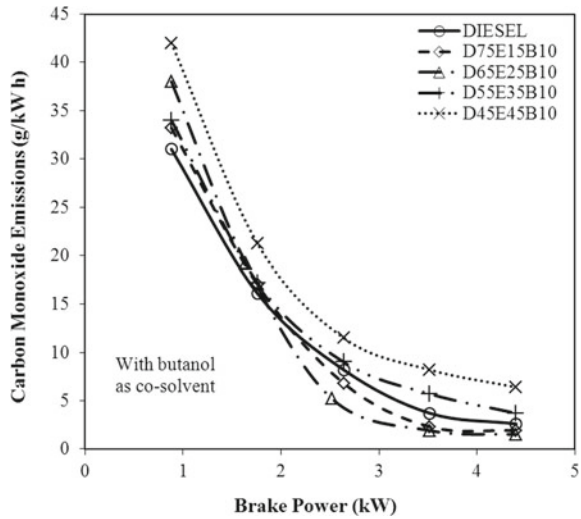


improves the evaporation rate of the final blend, which leads to a shorter duration for combustion, thereby offering higher temperature.

This enhances the fuel blend to produce lesser smoke emissions compared to diesel and other blends. However, addition of ethanol higher 25% increases the heat of vaporization of the final blend which suppresses the combustion temperature and hence offers lower in-cylinder temperature. This lower temperature reduces the reactivity of oxygen in the in-cylinder, which results in higher smoke emissions. This is the main reason for the higher smoke emissions from D55E35B10 and D45E45B10 compared to diesel. Carbon monoxide emissions from any CI engine are an indication of efficiency of combustion, degree of temperature of the in-cylinder during combustion, availability of oxygen for combustion, and self-ignition property of the fuel utilized in the engine. The present work utilized 15, 25, 35, and 45% of ethanol which possesses higher heat of vaporization.

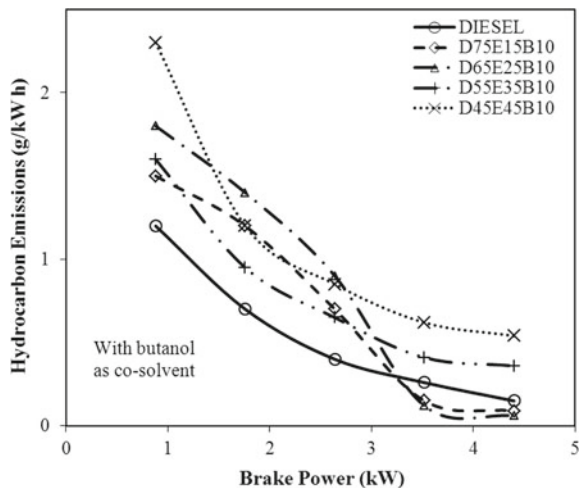
Hence, this volume of ethanol offers lower temperature in the in-cylinder resulting in higher CO emissions from the blends containing higher volume of ethanol compared to diesel. From Fig. 6.15, it can be seen that blends containing lower volume of ethanol produce lower CO emissions and blends containing high volume of ethanol produce higher CO emissions. This is mainly due to the improvement in the physical and chemical properties of the blend containing lower volume of ethanol (up to 25%) which reduces the CO emissions to a greater extent. Lower volume of ethanol improves the volatility and better atomization of the final blend, which enhances complete combustion and gives out lesser CO emissions compared to diesel. However, addition of ethanol higher than 25% to diesel increases the heat of vaporization to a greater extent which produces a cooling effect in the in-cylinder and hence produces higher CO emissions. This is also due to the slow rate of reactivity of oxygen with fuel during the combustion D75E15B10 and D65E25B10 produce lower CO emissions and D55E35B10 and D45E45B10 produce higher CO

Fig. 6.15 Variation of CO emissions versus brake power



emissions compared to diesel. The decreases of CO emissions from D75E15B10 and D65E25B10 are found to be lower by 27% and 46.1%, respectively, at rated power in comparison with diesel. The increases in CO emissions from D55E35B10 and D45E45B10 are found to be 37.2% and 58.2%, respectively, at rated power in comparison with diesel. This emission from any CI engine is also an indication of incomplete combustion, as the combustion in the available hydrocarbon in the fuel to carbon dioxide and water as products of complete combustion in the in-cylinder. From Fig. 6.16, it can be seen that containing 15% of ethanol offers lower HC emissions compared to diesel. This is mainly due to the increase in

Fig. 6.16 Variations of HC emissions of fuel blends



physico-chemical properties of the blends containing lower volume of ethanol and decrease in combustion characteristics of the blends containing higher volume of ethanol. The flame quenching at the vicinity of the cylinder walls and poor penetration at the crevice volume and the cylinder corners are the reasons for the higher HC emissions. Figure 6.16 shows that D75E15B10 and D65E25B10 produce 28 and 7.6% lower than diesel. The blend containing 45% of ethanol offers higher HC emissions compared to those produced by other blends. However, D55E35B10 and D45E45B10 produce significantly higher emissions compared to diesel at load conditions. However, D55E35B10 and D45E45B10 offer 8.2 and 12.6% lower in-cylinder pressure compared to diesel at full load compared to those produced at low load conditions. Also it can be observed that the start of pressure rise of all fuel blends is away from that of diesel. This is due to low cetane number of the final blend compared to diesel with respect to top dead center. The previous phase of the present study indicated that D45E45B10 blend is the possible volume of ethanol which has failed to produce better performance and emission characteristics. As the blends are producing comparatively low performance the option available to is modify the existing engine operating parameters to fuel the fuel blend in the existing engine. Also in the first phase, this blend has not suffered phase separation which is the major limitation of utilizing ethanol diesel blends in CI engine up to a lower temperature of 5 °C. The suitable parameters for fuelling CI engine by D45E45B10 have been determined by Taguchi method on ANOM approach (analysis of mean). This part of the work used Taguchi method for designing experimental layout and rank matrix to attain optimum level of parameters. The steps involved in the optimization process are as follows: (1) selection of operating parameters and their levels (2) selection of orthogonal array by Taguchi method (3) preparation of experimental layout (4) conducting the experiments using the experimental layout (5) observation of response parameters (6) listing the results and formation of rank matrix (7) suggesting optimal level of parameters, and (8) conducting engine experiment using optimal parameters.

Present investigation has considered four operating parameters, viz. injection pressure (IP), injection timing (IT), compression ratio (CR), and intake air temperature (IAT) for optimization. The range and level of parameters are decided with literature support and preliminary engine experiments. Table 6.6 shows the level of operating parameters. Using these parameters and their levels, a suitable orthogonal array, experimental layout, and number trials of the experiments have been arrived from Taguchi method of optimization.

Taguchi method of optimization offers a systematic approach to arrive at the level of performance parameters involved in the response parameters. The Taguchi method uses an orthogonal array for designing the experimental layout. The selection of orthogonal array is arrived from the degrees of freedom of the parameters involved (Rakopoulos et al. 2008). The minimum number of experiments (trials) for selecting the optimum level of parameters can be determined using the relation:

$$N = (L - 1) * P + 1 \quad (6.4)$$

Table 6.5 Instruments used with accuracies and uncertainties

S. No.	Instruments	Range	Accuracy	Percentage of uncertainties
1	Smoke level measuring instrument	BSU 0–10	+ 0.1 to –0.1	±1
2	Exhaust gas temperature indicator	0–900 °C	+1 to –1 °C	±0.15
3	Speed measuring unit	0–10,000 rpm	+10 to –10 rpm	±0.1
4	Burette for fuel measurement		+0.1 to –0.1 cc	±1
5	Digital stopwatch		+0.6 to – 0.6 s	±0.2
6	Manometer		+1 to –1 mm	±1
7	Pressure pickup	0–110 bar	+ 0.1 to –0.1 kg	±0.1
8	Crank angle encoder		+1° to –1°	±0.2

where N = total number of test runs, L = number of levels of parameters, and P = number of control parameters.

The present study uses (Table 6.5) four parameters and three levels, and hence, the total degrees of freedom of control parameters are 8. Therefore, L_9 is suitable OA for the total degrees of freedom of involved parameters.

Analysis of Mean (ANOM) This is used after attaining the experimental results as per the L_9 orthogonal array of nine experiments containing three sets of reading in each setting. A rank matrix table is utilized for the analysis of captured data. A rank matrix Table 6.8 has been constructed to arrive at the optimal level of parameters. Average of the sum of the each level outcome has been obtained, and the rank is tabulated for the maximum of the outcome.

Assuming that Y as output parameter and the level summation has been obtained as follows:

$$A_1 = Y_1 + Y_2 + Y_3 \text{ (in which the level 1 is denoted in the orthogonal array)} \quad (6.5)$$

Similar calculation has been done for three levels and for four parameters, from which the rank matrix table has been constructed.

Table 6.6 Parameters involved in the optimization and their levels

S. No.	Symbol	Parameters	Level 1	Level 2	Level 3
1	A	Injection pressure (IP) (bar)	190	200	210
2	B	Injection timing (IT) (°BTDC)	26	29	32
3	C	Compression ratio (CR)	17.5	19	21
4	D	Intake air temperature(IAT) (°C)	50	75	100

Table 6.7 L_9 orthogonal array

Trial No.	Column No.			
	A	B	C	D
1	1	1	1	1
2	1	2	2	2
3	1	3	3	3
4	2	1	2	3
5	2	2	3	1
6	2	3	1	2
7	3	1	3	2
8	3	2	1	3
9	3	3	2	1

Table 6.8 Rank matrix (for BTE)

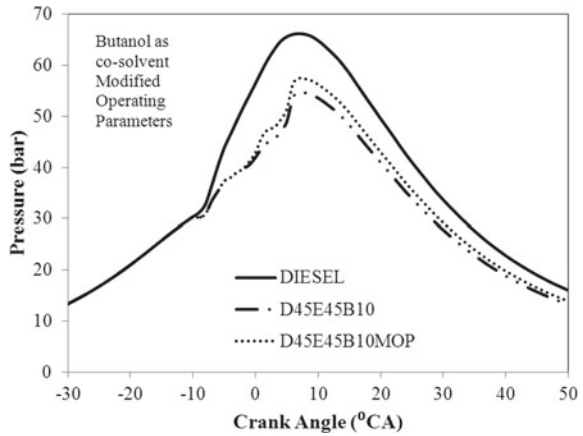
Rank	A_1 (Level 1)	B_2 (Level 3)	C_3 (Level 3)	D_4 (Level 3)
Level/Parameter	A	B	C	D
1	31.3	31.6	30.6	30
2	31.05	29.86	31.36	31.6
3	31.1	31.96	31.66	31.7

From Table 6.7, it can be concluded that IP 190 bar (LEVEL1), IT 29 °bTDC (LEVEL3), CR 19 (LEVEL3), and IAT 100 (LEVEL3) are the optimal parameters by comparing the rank.

The same sets of readings are captured for NO_x to match with the brake thermal efficiency. The optimized levels of operating parameters are as shown in Table 6.7. Blend D45E45B10 has been tested under the modified operating parameters, and the results are compared with diesel and D45E45B10 under normal operating parameters. The same engine has been used for the testing of the blends under modified operating parameters. The results of the experiment are presented in graphical form. The variations of cylinder pressure with crank angle at rated power for the blend D45E45B10 under standard operating parameters and modified operating parameters are presented in Fig. 6.17, and it is seen that the modified engine operating parameters increased the cylinder pressure significantly compared to diesel. This is due to the increased heat energy release in the combustion chamber with increase in compression ratio and intake air temperature.

Also, the advancement in the injection timing improves the pre-combustion phase and results in more complete combustion. This shows the suitability of the modified engine operating parameters for the blend D45E45B10. The increase in pressure of D45E45B10MOP is found as 7.1% higher than diesel at rated power. However, the cylinder pressure is found lesser than diesel. This is due to the lesser essential properties of D45E45B10 in comparison with diesel. Variation of in-cylinder

Fig. 6.17 Variation of cylinder pressure with crank angle at rated power



peak pressure versus brake power for D45E45B10 under modified engine operating parameters is shown in Fig. 6.18. It is seen that the in-cylinder peak pressure increases by fuelling D45E45B10 under modified operating parameters compared to that of normal operating parameters. This is due to the suitability of the modified operating parameters for the blend D45E45B10. Also, the increase in the in-cylinder peak pressure is found proportional to the increase in brake power. This increase is due to the improved rate of combustion by the increase in compression ratio and intake air temperature. Also, the advancement of injection timing improved the pre-combustion phase which suppresses the dominance of heat of vaporization of the blend. However, the in-cylinder peak pressure of D45E45B10MOP is found lesser than diesel at all load conditions. This is due to the lesser energy content of D45E45B10 in comparison with diesel. The increase in the in-cylinder peak pressure of D45E45B10MOP is

Fig. 6.18 Variation of in-cylinder peak pressure versus brake power

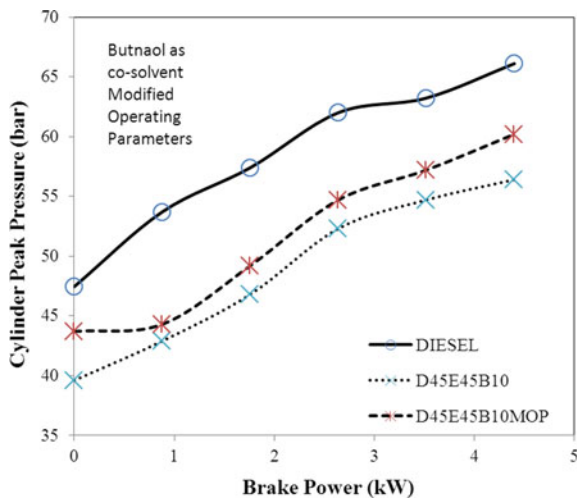
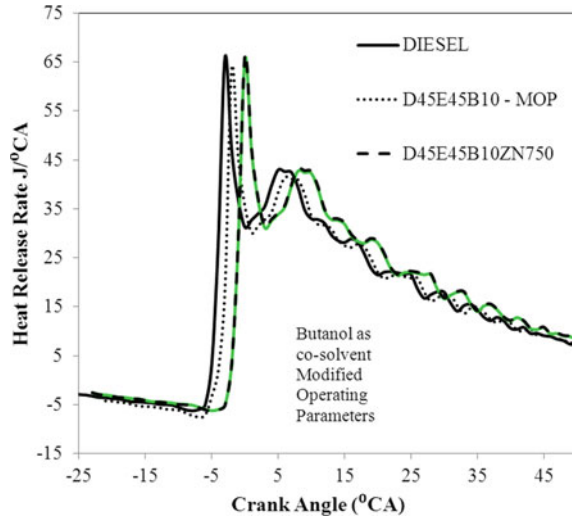


Fig. 6.19 Variation of HRR with crank angle at rated power



found as 6.3% higher than D45E45B10. Heat release rate is an indicator of combustion efficiency, and these parameters are helping for explaining the BTE, exhaust gas temperature, rate of pressure rise, emission parameters, and cylinder pressure.

Figure 6.19 shows the variation of HRR of fuel blends with 10% butanol as co-solvent without any modification under full load condition. HRR graphs are generated at all loads, and for representation HRR at full load condition is presented. It can be seen from figure that ethanol addition up to 25% increases the HRR to a greater extent due to the enhanced combustion behavior resulted from better atomization. However, the increase in ethanol content beyond 25% decreases HRR of the blends as poor atomization resulting in lesser heat release rate. From Fig. 6.19, it is also seen that the blends containing lower ethanol offer higher HRR and blends containing higher ethanol offer lower HRR. The peak HRR of the blends occur an angle away from that of diesel. The combustion duration of the blends containing lower ethanol is shorter than that of blends containing higher ethanol content.

The increases of HRR of D65E15B10 and D55E25B10 are 8.8% and 12.9% higher than diesel. From Fig. 6.20, it is observed that the target blend D45E45B10 offers higher BTE with modified operating parameters compared to that of BTE with normal operating parameters. However, this blend offers lesser BTE compared to that of diesel. The reason for the increase in BTE is due to the increase in heat content of the combustion chamber resulted from the enhanced combustion triggered by the modified operating parameters. Ignition quality decreases the combustion temperature and thereby lesser BTE compared to diesel. Similar observation was presented by previous researchers (Verma et al. 2018) (Fig. 6.20).

The increase in BTE by the modification of operating parameters is 6.7% compared to those in normal operating parameters, which indicates the suitability of the parameters for the target blend. The decrease in BTE of the target blend at modified operating parameters is only 2.1% compared to diesel. Variation of EGT with

Fig. 6.20 Variation of brake thermal efficiency versus brake power

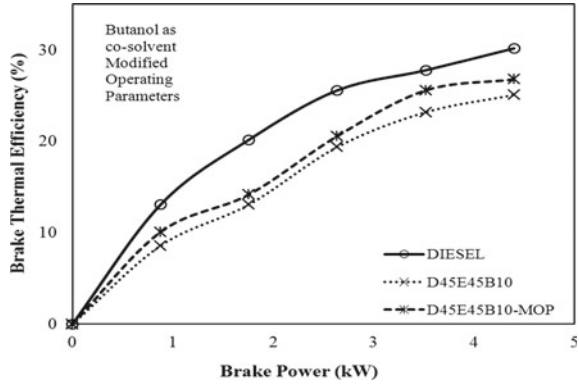
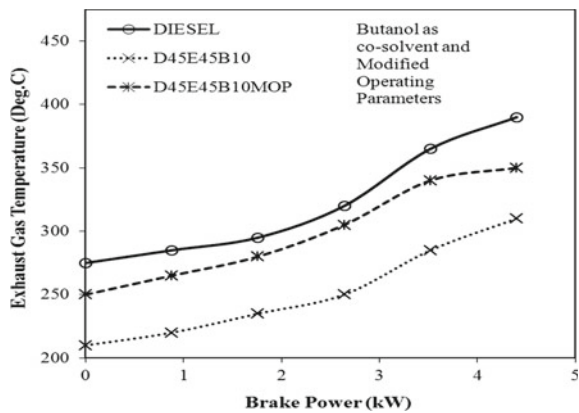


Fig. 6.21 Variation of EGT versus brake power



respect to brake power is as shown in Fig. 6.21. The quantity of ethanol in the blend determines the performance of the blend as the increase in ethanol volume results in poor to brake power for the blend D45E45B10 operated under normal operating parameters and modified operating parameters in comparison with diesel. It is seen that there is a significant increase in EGT of D45E45B10MOP in all load conditions compared to those under normal operating parameters. This is due to the higher heat energy release by the blend operated under modified operating parameters. This is due to the suppression of the dominance created by the heat of vaporization of the higher volume of ethanol by the modified parameters to a certain extent. However, the EGT of D45E45B10MOP is found lesser than diesel. The increase of EGT of D45E45B10MOP is found 13.1% higher than D45E45B10 at rated power. This is due to the increase in heat content of the target blend operating with modified operating parameter and compressed air, which helps to combust the fuel by reducing the ignition delay. However, the emissions of NO_x are lesser than diesel as the higher volume of ethanol suppresses the temperature of the in-cylinder. The increase in NO_x

emissions due to the modification of operating parameters is 100% (approximately double) compared to that of operating under normal operating parameters.

The decrease in NO_x emissions of D45E45B10 –MOP is 40.5% compared to that of diesel at full load condition. Figure 6.23 shows the smoke opacity of the target blend under modified operating parameters at all load conditions. It can be observed that there is a significant reduction in smoke emissions from the target blend under modified operating parameters compared to that under normal operating parameters.

This is due to the reason of increased temperature of the in-cylinder by the modified operating parameters which enhances higher heat release resulted from compressed

Fig. 6.22 Variation of NO_x emissions versus brake power

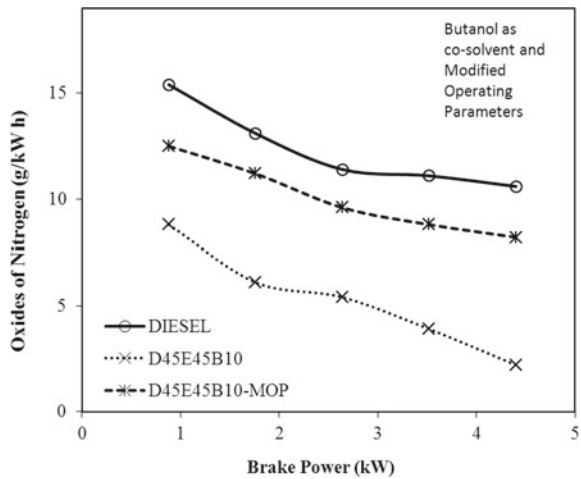


Fig. 6.23 Variation of smoke opacity versus brake power

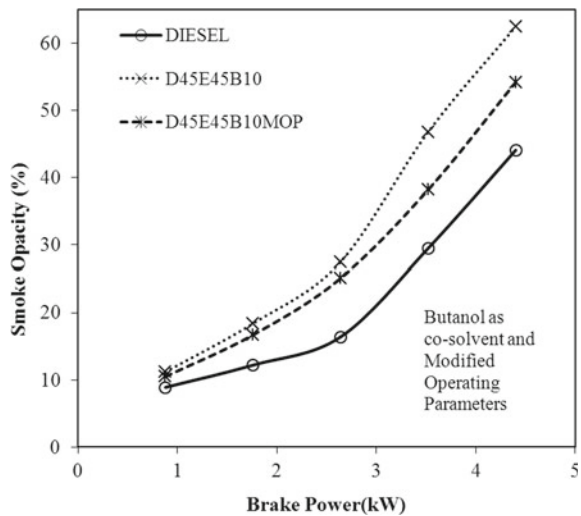
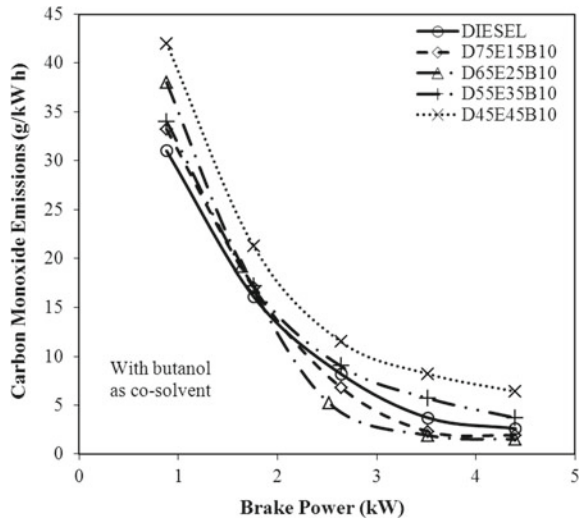


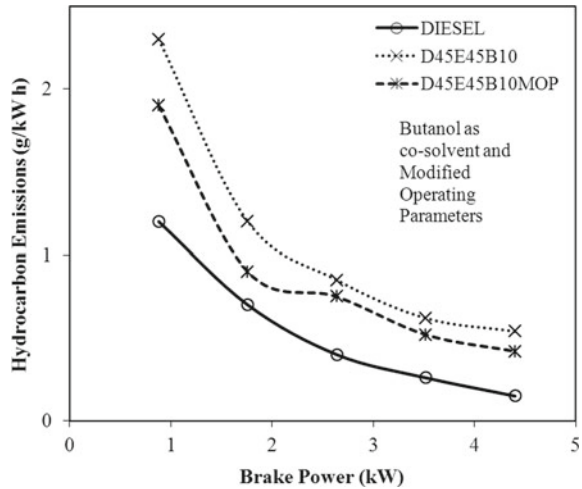
Fig. 6.24 Variations of CO emissions versus brake power



air. However, the higher heat of vaporization of the blend still suppresses the temperature, and hence, there is an increase in smoke emissions compared to that of diesel. The decrease in smoke emissions is 21.2% compared to D45E45B10 operated under normal operating parameters. The increase in smoke emissions of D45E45B10-MOP is 16.5% higher than diesel at full load condition. Similar results were observed by previous researchers (Ghadikolaei et al. 2018). From Fig. 6.24, it can be seen that there is a significant reduction of CO emissions due to the modification of operating parameters to the target blend.

This is due to impact of the modified parameters on the combustion characteristics to a certain extent. However, the higher ethanol content increases the heat of vaporization of the final blend, which results in poor ignition quality which results in lesser temperature of the in-cylinder shows the variation of CO emissions of D45E45B10 fuelled in the test engine under modified operating parameters compared to that of diesel. This reduces the BTE of the blend lesser than diesel. The increase in BTE of the blend at modified operating parameters is 29.6% compared to that operated under normal operating parameters. However, the increase in CO of the blend is 19.3% higher than diesel. Higher ethanol content affects the self-ignition property; hence, it reduces reaction rate, combustion temperature, and heat release rate (Rakopoulos et al. 2008). Figure 6.25 presents the HC emissions of D45E45B10 under modified operating parameters along with diesel for comparison. It is seen that there is a significant reduction in HC emissions from the target blend. This is due to the increase heat content of the combustion chamber and compressed air by the modified parameters which results in better reactivity of the available oxygen with fuel.

Fig. 6.25 Variation of HC emissions versus brake power



6.4 Conclusion

Different phases of study have been followed to utilize diesel ethanol blends as fuel in compression ignition (CI) engine in this study. Experiments have been conducted with diesel ethanol without co-solvent and with butanol as co-solvent. The effects of engine operating parameters such as injection pressure (IP), injection timing (IT), compression ratio (CR), and intake air temperature (IAT) on engine performance, combustion, and emission were studied.

- Results of the solubility test indicate that ethanol can be blended with diesel up to a volume of 50% with 10% butanol as co-solvent. This blend is found as stable up to a lower temperature of 5 °C for 20 days.
- Results of property testing show those properties of the blend containing 45% of ethanol and 10% butanol as co-solvent are found suitable for replacing diesel to fuel CI engine. However, blend containing 50% ethanol and 10% butanol is found not suitable as the cetane number is less than 30 which is a minimum requirement as per ASTM standards.
- The D80E20 shows higher peak pressure of 72.2 bar compared to D90E10I and diesel showing 68 bar and 66.4 bar, respectively, at rated power due to improved physico-chemical properties, better ignition quality, improved air–fuel mixing, and higher oxygen content. D80E20 shows higher HRR of 71.2 J/° CA compared to diesel and D90E10 at rated power. The brake thermal efficiency of D80E10 (31.8%) is higher than that of diesel (30.2%). Increase the NO_x emission by 13.2% in the case of D80E20, whereas 2.9% increase is observed for D90E10 compared with diesel.
- The lower cetane number of D45E45B10 retards the combustion by 4 °CA compared to diesel operation. The peak pressure is lower for D45E45B10 in the entire load range when compared to diesel operation. This blend shows a

significantly lower brake thermal efficiency compared to diesel operation and is found 16.8% lesser than diesel at rated power.

- The NO_x emission for D45E45B10 is 22.5% lesser, and the increase in smoke emission is about 49.2% compared to diesel. HC is increased by 6.7% in the case of D45E45B10 operation compared to diesel operation. The CO emission follows the same trend as that of HC emission. Although this phase gave adverse effects in performance and emissions, higher volume of ethanol is utilized without any phase separation.
- D45E45B10MOP operation advances the combustion and improves premixed combustion compared to D45E45B10 under normal operating parameters. However, D45E45B10 shows lower peak heat release rate and peak pressure at rated power compared to diesel operation. This blend produced an increase in BTE at rated power is 6.8% higher than D45E45B10 fuelled under normal operating parameters. However, BTE of D45E45B10MOP is found lesser than diesel at rated power. An increase in NO_x emission by fueling D45E45B10MOP operation is found compared to D45E45B10. The increase in NO_x emissions of D45E45B10MOP is found thrice that of NO_x emissions from D45E45B10 fuelled under normal operating parameters. However, NO_x emissions of D45E45B10MOP are found lesser than diesel at rated power.
- The smoke emission is reduced by 15.4% in fueling D45E45B10MOP compared to D45E45B10 fuelled under normal operating parameters. The HC and CO emissions are reduced by 22.5% and 9.2%, respectively, in fuelling D45E45B10MOP compared to D45E45B10 fuelled under normal operating parameters.

As a sum up, although the efficiency produced by D45E45B10 is found to be marginally lower and the emissions of smoke, and HC and CO produced are found to be marginally higher compared to that of diesel. The utilized ethanol and butanol are manufactured from waste products, and the emissions of oxides of nitrogen produced are found to be significantly lower compared to that of diesel. Hence, higher volume of ethanol can be utilized and a saving of 55% of diesel fuel can be achieved by the implementation of this modification in fuel and in engine. This in turn reduces the dependency of other countries for import of crude oil.

References

- Belgiorno G, Di Blasio G, Shamun S, Beatrice C, Tunestål P, Tunér M (2018) Performance and emissions of diesel-gasoline-ethanol blends in a light duty compression ignition engine. *Fuel* 217:78–90
- Gao Z, Lin S, Ji J, Li M (2019) An experimental study on combustion performance and flame spread characteristics over liquid diesel and ethanol-diesel blended fuel. *Energy* 170:349–355
- Ghadikolaie MA, Cheung CS, Yung KF, (2018) Study of combustion, performance and emissions of diesel engine fueled with diesel/biodiesel/alcohol blends having the same oxygen concentration. *Energy*
- Gnanamoorthi V, Devaradjane G (2015) Effect of compression ratio on the performance, combustion and emission of DI diesel engine fueled with ethanol–diesel blend. *J Energy Inst* 88(1):19–26

- Hafid HS, Shah UKM, Baharuddin AS, Ariff AB (2017) Feasibility of using kitchen waste as future substrate for bioethanol production: a review. *Renew Sustain Energy Rev* 74:671–686
- Han J, Somers LMT, Cracknell R, Joedicke A, Wardle R, Mohan VRR (2020) Experimental investigation of ethanol/diesel dual-fuel combustion in a heavy-duty diesel engine. *Fuel* 275:117867
- Hansen AC, Zhang Q, Lyne PW (2005) Ethanol–diesel fuel blends—A review. *Biores Technol* 96(3):277–285
- Holman JP, Gajda WJ (2001) *Experimental methods for engineers*, vol 2. McGraw-Hill, New York
- Kumar S, Cho JH, Park J, Moon I (2013) Advances in diesel–alcohol blends and their effects on the performance and emissions of diesel engines. *Renew Sustain Energy Rev* 22:46–72
- Kuszewski H (2018) Experimental investigation of the effect of ambient gas temperature on the autoignition properties of ethanol–diesel fuel blends. *Fuel* 214:26–38
- Mamat R, Sani MSM, Sudhakar K, Kadarohman A, Sardjono RE (2019) An overview of Higher alcohol and biodiesel as alternative fuels in engines. *Energy Rep* 5:467–479
- Pinzi S, López I, Leiva-Candia DE, Redel-Macías MD, Herreros JM, Cubero-Atienza A, Dorado MP (2018) Castor oil enhanced effect on fuel ethanol-diesel fuel blend properties. *Appl Energy* 224:409–416
- Prabakaran B, Vijayabalan P (2016) Evaluation of the performance of n-butanol-ethanol-diesel blends in a diesel engine. *Int J Energy Clean Environ* 17:81–97
- Prabakaran B, Vijayabalan P, Balachandar M. (2017) Experimental Investigation of ethanol-diesel-butanol blends in a compression ignition engine by modifying the operating parameters. *SAE Int J Eng* 11(03-11-05-0037)
- Prabakaran B, Vijayabalan P, Balachandar M (2019) An assessment of diesel ethanol blend fueled diesel engine characteristics using butanol as cosolvent for optimum operating parameters. *Energy Sources Part A-Recov Util Environ Effects*
- Rakopoulos DC, Antonopoulos KA, Rakopoulos DC, Hountalas DT (2008) Multi-zone modeling of combustion and emissions formation in DI diesel engine operating on ethanol–diesel fuel blends. *Energy Convers Manage* 49(4):625–643
- Rakopoulos DC, Rakopoulos CD, Giakoumis EG, Papagiannakis RG, Kyritsis DC (2014) Influence of properties of various common bio-fuels on the combustion and emission characteristics of high-speed DI (direct injection) diesel engine: vegetable oil, bio-diesel, ethanol, *n*-butanol, diethyl ether. *Energy* 73:354–366
- Rakopoulos CD, Rakopoulos DC, Kosmadakis GM, Papagiannakis RG (2019) Experimental comparative assessment of butanol or ethanol diesel-fuel extenders impact on combustion features, cyclic irregularity, and regulated emissions balance in heavy-duty diesel engine. *Energy* 174:1145–1157
- Ribeiro NM, Pinto AC, Quintella CM, da Rocha GO, Teixeira LS, Guarieiro LL, do Carmo Rangel M, Veloso MC, Rezende MJ, Serpa da Cruz R, de Oliveira AM (2007) The role of additives for diesel and diesel blended (ethanol or biodiesel) fuels: a review. *Energy Fuels* 21(4):2433–2445
- Shamun S, Belgiorno G, Di Blasio G, Beatrice C, Tunér M, Tunestål P (2018) Performance and emissions of diesel-biodiesel-ethanol blends in a light duty compression ignition engine. *Appl Thermal Eng* 145:444–452
- Singh GN, Bharj RS (2019) Study of physical-chemical properties for 2nd generation ethanol-blended diesel fuel in India. *Sustain Chem Pharm* 12:100130
- Stoeberl M, Werkmeister R, Faulstich M, Russ W (2011) Biobutanol from food wastes—fermentative production, use as biofuel and the influence on the emissions. *Procedia Food Sci* 1:1867–1874
- Verma S, Sharma B, Ahmad J, Dwivedi G, Nandan G (2018) Impact assessment of ethanol as fuel for engine operation. *Mater Today: Proceed* 5(2):6115–6120
- Woo C, Kook S, Hawkes ER (2016) Effect of intake air temperature and common-rail pressure on ethanol combustion in a single-cylinder light-duty diesel engine. *Fuel* 180:9–19

Yilmaz N (2012) Comparative analysis of biodiesel–ethanol–diesel and biodiesel–methanol–diesel blends in a diesel engine. *Energy* 40(1):210–213

Yu Y (2019) Experimental study on effects of ethanol-diesel fuel blended on spray characteristics under ultra-high injection pressure up to 350 MPa. *Energy* 186:115768